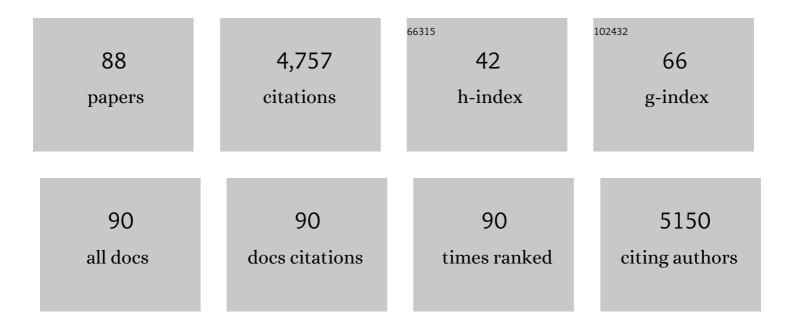
Yongsheng Yu

List of Publications by Year in descending order

Source: https://exaly.com/author-pdf/4266653/publications.pdf Version: 2024-02-01



YONCSHENC YU

#	Article	IF	CITATIONS
1	A New Core/Shell NiAu/Au Nanoparticle Catalyst with Pt-like Activity for Hydrogen Evolution Reaction. Journal of the American Chemical Society, 2015, 137, 5859-5862.	6.6	274
2	Exclusive Strain Effect Boosts Overall Water Splitting in PdCu/Ir Core/Shell Nanocrystals. Angewandte Chemie - International Edition, 2021, 60, 8243-8250.	7.2	163
3	Monodisperse MPt (M = Fe, Co, Ni, Cu, Zn) Nanoparticles Prepared from a Facile Oleylamine Reduction of Metal Salts. Nano Letters, 2014, 14, 2778-2782.	4.5	156
4	Building P-doped MoS2/g-C3N4 layered heterojunction with a dual-internal electric field for efficient photocatalytic sterilization. Chemical Engineering Journal, 2022, 429, 132588.	6.6	138
5	Controlled Anisotropic Growth of Coâ€Feâ€P from Coâ€Feâ€O Nanoparticles. Angewandte Chemie - International Edition, 2015, 54, 9642-9645.	7.2	132
6	One-pot synthesis of magnetic graphene oxide composites as an efficient and recoverable adsorbent for Cd(II) and Pb(II) removal from aqueous solution. Journal of Hazardous Materials, 2020, 381, 120914.	6.5	126
7	Photocatalytic dehydrogenation of formic acid promoted by a superior PdAg@g-C ₃ N ₄ Mott–Schottky heterojunction. Journal of Materials Chemistry A, 2019, 7, 2022-2026.	5.2	116
8	Activating interfacial S sites of MoS2 boosts hydrogen evolution electrocatalysis. Nano Research, 2022, 15, 1809-1816.	5.8	111
9	Efficient photocatalytic reduction of Cr(VI) in aqueous solution over CoS2/g-C3N4-rGO nanocomposites under visible light. Applied Surface Science, 2020, 510, 145495.	3.1	108
10	Hierarchical core-shell electrode with NiWO4 nanoparticles wrapped MnCo2O4 nanowire arrays on Ni foam for high-performance asymmetric supercapacitors. Journal of Colloid and Interface Science, 2020, 563, 405-413.	5.0	103
11	Fe3O4 nanoparticles coated with ultra-thin carbon layer for polarization-controlled microwave absorption performance. Journal of Colloid and Interface Science, 2021, 600, 382-389.	5.0	99
12	Cobaltâ€ S ubstituted Magnetite Nanoparticles and Their Assembly into Ferrimagnetic Nanoparticle Arrays. Advanced Materials, 2013, 25, 3090-3094.	11.1	95
13	One-Pot Synthesis of Urchin-like FePd–Fe3O4 and Their Conversion into Exchange-Coupled L10–FePd–Fe Nanocomposite Magnets. Nano Letters, 2013, 13, 4975-4979.	4.5	87
14	Subâ€Monolayer YO <i>_x</i> /MoO <i>_x</i> on Ultrathin Pt Nanowires Boosts Alcohol Oxidation Electrocatalysis. Advanced Materials, 2021, 33, e2103762.	11.1	86
15	L-Cysteine capped Mo2C/Zn0.67Cd0.33S heterojunction with intimate covalent bonds enables efficient and stable H2-Releasing photocatalysis. Chemical Engineering Journal, 2022, 428, 132628.	6.6	85
16	Interface engineering: PSS-PPy wrapping amorphous Ni-Co-P for enhancing neutral-pH hydrogen evolution reaction performance. Chemical Engineering Journal, 2021, 417, 129232.	6.6	82
17	Highly efficient recovery of heavy rare earth elements by using an amino-functionalized magnetic graphene oxide with acid and base resistance. Journal of Hazardous Materials, 2022, 424, 127370.	6.5	82
18	Porous layered stacked MnCo ₂ O ₄ cubes with enhanced electrochemical capacitive performance. Nanoscale, 2018, 10, 2218-2225.	2.8	80

#	Article	IF	CITATIONS
19	Schiff-base-rich g-CxN4 supported PdAg nanowires as an efficient Mott–Schottky catalyst boosting photocatalytic dehydrogenation of formic acid. Rare Metals, 2021, 40, 808-816.	3.6	77
20	Lavender-Like Ga-Doped Pt ₃ Co Nanowires for Highly Stable and Active Electrocatalysis. ACS Catalysis, 2020, 10, 3018-3026.	5.5	75
21	Highly efficient and ultrafast removal of Cr(VI) in aqueous solution to ppb level by poly(allylamine) Tj ETQq1 Materials, 2021, 409, 124470.	. 0.784314 r 6.5	gBT /Overloc 75
22	High-performance asymmetric supercapacitors based on monodisperse MnO nanocrystals with high energy densities. Nanoscale, 2018, 10, 15926-15931.	2.8	74
23	Shortâ€Range Diffusion Enables General Synthesis of Mediumâ€Entropy Alloy Aerogels. Advanced Materials, 2022, 34, .	11.1	74
24	Room-Temperature Chemoselective Reduction of 3-Nitrostyrene to 3-Vinylaniline by Ammonia Borane over Cu Nanoparticles. Journal of the American Chemical Society, 2018, 140, 16460-16463.	6.6	73
25	A general strategy for bimetallic Pt-based nano-branched structures as highly active and stable oxygen reduction and methanol oxidation bifunctional catalysts. Nano Research, 2020, 13, 638-645.	5.8	70
26	Carbon-coated defect-rich MnFe2O4/MnO heterojunction for high-performance microwave absorption. Carbon, 2022, 194, 207-219.	5.4	68
27	Comparison of the Stem-Loop and Linear Probe-Based Electrochemical DNA Sensors by Alternating Current Voltammetry and Cyclic Voltammetry. Langmuir, 2011, 27, 14669-14677.	1.6	66
28	Hole-rich CoP nanosheets with an optimized d-band center for enhancing pH-universal hydrogen evolution electrocatalysis. Journal of Materials Chemistry A, 2021, 9, 8561-8567.	5.2	66
29	Ni nanoparticles supported on graphitic carbon nitride as visible light catalysts for hydrolytic dehydrogenation of ammonia borane. Nanoscale, 2019, 11, 3506-3513.	2.8	61
30	3D ordered mesoporous cobalt ferrite phosphides for overall water splitting. Science China Materials, 2020, 63, 240-248.	3.5	61
31	Nitrogen-rich g-C3N4@AgPd Mott-Schottky heterojunction boosts photocatalytic hydrogen production from water and tandem reduction of NO3â^ and NO2â^. Journal of Colloid and Interface Science, 2021, 581, 619-626.	5.0	58
32	Engineering defects and adjusting electronic structure on S doped MoO2 nanosheets toward highly active hydrogen evolution reaction. Nano Research, 2020, 13, 121-126.	5.8	57
33	Three-dimensional foam-like Fe3O4@C core-shell nanocomposites: Controllable synthesis and wideband electromagnetic wave absorption properties. Journal of Magnetism and Magnetic Materials, 2020, 502, 166518.	1.0	57
34	Z-Scheme Mo ₂ C/MoS ₂ /In ₂ S ₃ dual-heterojunctions for the photocatalytic reduction of Cr(<scp>vi</scp>). Journal of Materials Chemistry A, 2021, 9, 10297-10303.	5.2	56
35	Direct chemical synthesis of L1 ₀ -FePtAu nanoparticles with high coercivity. Nanoscale, 2014, 6, 12050-12055.	2.8	53
36	Engineering sulfur vacancies in basal plane of MoS2 for enhanced hydrogen evolution reaction. Journal of Catalysis, 2020, 391, 91-97.	3.1	52

#	Article	IF	CITATIONS
37	Halide Ion-Mediated Synthesis of L1 ₀ -FePt Nanoparticles with Tunable Magnetic Properties. Nano Letters, 2018, 18, 7839-7844.	4.5	51
38	A highly sensitive sensor based on ordered mesoporous ZnFe2O4 for electrochemical detection of dopamine. Analytica Chimica Acta, 2020, 1096, 26-33.	2.6	49
39	Enhancing electrochemical detection of dopamine via dumbbell-like FePt–Fe ₃ O ₄ nanoparticles. Nanoscale, 2017, 9, 1022-1027.	2.8	48
40	Structural Regulation of Pdâ€Based Nanoalloys for Advanced Electrocatalysis. Small Science, 2021, 1, 2100061.	5.8	48
41	Hierarchical mesoporous Co3O4@ZnCo2O4 hybrid nanowire arrays supported on Ni foam for high-performance asymmetric supercapacitors. Science China Materials, 2018, 61, 1167-1176.	3.5	45
42	Controlled synthesis and assembly into anisotropic arrays of magnetic cobalt-substituted magnetite nanocubes. Nanoscale, 2015, 7, 2877-2882.	2.8	44
43	Ordered mesoporous spinel CoFe2O4 as efficient electrocatalyst for the oxygen evolution reaction. Journal of Electroanalytical Chemistry, 2019, 840, 409-414.	1.9	44
44	Folding-based electrochemical DNA sensor fabricated on a gold-plated screen-printed carbon electrode. Chemical Communications, 2009, , 2902.	2.2	43
45	Enhanced electron transfer and light absorption on imino polymer capped PdAg nanowire networks for efficient room-temperature dehydrogenation of formic acid. Journal of Materials Chemistry A, 2018, 6, 1979-1984.	5.2	43
46	Amino-assisted AHMT anchored on graphene oxide as high performance adsorbent for efficient removal of Cr(VI) and Hg(II) from aqueous solutions under wide pH range. Journal of Hazardous Materials, 2021, 416, 125825.	6.5	43
47	Designing shape anisotropic SmCo ₅ particles by chemical synthesis to reveal the morphological evolution mechanism. Nanoscale, 2018, 10, 10377-10382.	2.8	42
48	Monodisperse PtCu alloy nanoparticles as highly efficient catalysts for the hydrolytic dehydrogenation of ammonia borane. International Journal of Hydrogen Energy, 2018, 43, 14293-14300.	3.8	42
49	Chemical Synthesis of Magnetically Hard and Strong Rare Earth Metal Based Nanomagnets. Angewandte Chemie - International Edition, 2019, 58, 602-606.	7.2	42
50	From FePt–Fe ₃ O ₄ to L1 ₀ -FePt–Fe nanocomposite magnets with a gradient interface. Journal of Materials Chemistry C, 2015, 3, 7075-7080.	2.7	41
51	Surface Pd-rich PdAg nanowires as highly efficient catalysts for dehydrogenation of formic acid and subsequent hydrogenation of adiponitrile. Journal of Materials Chemistry A, 2018, 6, 17323-17328.	5.2	41
52	High-density defects on PdAg nanowire networks as catalytic hot spots for efficient dehydrogenation of formic acid and reduction of nitrate. Nanoscale, 2017, 9, 9305-9309.	2.8	38
53	Amino-functionalized graphene oxide-supported networked Pd–Ag nanowires as highly efficient catalyst for reducing Cr(VI) in industrial effluent by formic acid. Chemosphere, 2020, 257, 127245.	4.2	38
54	A general strategy for synthesizing high-coercivity L1 ₀ -FePt nanoparticles. Nanoscale, 2017, 9, 12855-12861.	2.8	37

#	Article	lF	CITATIONS
55	Structural engineering of Fe-doped Ni2P nanosheets arrays for enhancing bifunctional electrocatalysis towards overall water splitting. Applied Surface Science, 2021, 536, 147909.	3.1	37
56	Modulating the surface segregation of PdCuRu nanocrystals for enhanced all-pH hydrogen evolution electrocatalysis. Journal of Materials Chemistry A, 2019, 7, 20151-20157.	5.2	36
57	Industrially promising NiCoP nanorod arrays tailored with trace W and Mo atoms for boosting large-current-density overall water splitting. Nanoscale, 2021, 13, 14179-14185.	2.8	36
58	Bifunctional networked Ag/AgPd core/shell nanowires for the highly efficient dehydrogenation of formic acid and subsequent reduction of nitrate and nitrite in water. Journal of Materials Chemistry A, 2018, 6, 4611-4616.	5.2	35
59	A dual-signalling electrochemical DNA sensor based on target hybridization-induced change in DNA probe flexibility. Chemical Communications, 2012, 48, 8703.	2.2	34
60	Highâ€Index Faceted PdPtCu Ultrathin Nanorings Enable Highly Active and Stable Oxygen Reduction Electrocatalysis. Small Methods, 2021, 5, e2100154.	4.6	34
61	Folding-based electrochemical DNA sensor fabricated by "click―chemistry. Chemical Communications, 2009, , 4835.	2.2	31
62	Facile synthesis of highly ordered mesoporous Fe3O4 with ultrasensitive detection of dopamine. Talanta, 2019, 201, 511-518.	2.9	30
63	Fabrication, characterization, and magnetic properties of exchange-coupled porous BaFe ₈ Al ₄ O ₁₉ /Co _{0.6} Zn _{0.4} Fe ₂ O nanocomposite magnets. Nanoscale, 2019, 11, 10629-10635.	< su bว_ิงส < /รเ	ub>29
64	Effect of diluent chain length on the performance of the electrochemical DNA sensor at elevated temperature. Analyst, The, 2011, 136, 134-139.	1.7	22
65	Cu induced low temperature ordering of fct-FePtCu nanoparticles prepared by solution phase synthesis. Journal of Materials Chemistry C, 2019, 7, 11632-11638.	2.7	22
66	A Bidentate Ru(II)-NC Complex as a Catalyst for Semihydrogenation of Alkynes to (<i>E</i>)-Alkenes with Ethanol. Organometallics, 2020, 39, 862-869.	1.1	21
67	Mesoporous cobalt ferrite phosphides/reduced graphene oxide as highly effective electrocatalyst for overall water splitting. Journal of Colloid and Interface Science, 2022, 605, 667-673.	5.0	21
68	Bi-doped graphitic carbon nitride nanotubes boost the photocatalytic degradation of Rhodamine B. New Journal of Chemistry, 2022, 46, 3588-3594.	1.4	20
69	Designing a novel dual Z-scheme Bi2S3-ZnS/MoSe2 photocatalyst for photocatalytic reduction of Cr(VI). Separation and Purification Technology, 2022, 286, 120502.	3.9	20
70	Disposable multiplexed electrochemical sensors based on electro-triggered selective immobilization of probes for simultaneous detection of DNA and proteins. Journal of Materials Chemistry B, 2020, 8, 7501-7510.	2.9	19
71	A facile solution phase synthesis of directly ordering monodisperse FePt nanoparticles. Nano Research, 2022, 15, 446-451.	5.8	19
72	Ceâ€Doped Ordered Mesoporous Cobalt Ferrite Phosphides as Robust Catalysts for Water Oxidation. Chemistry - A European Journal, 2020, 26, 13305-13310.	1.7	18

#	Article	IF	CITATIONS
73	Cross-linked sulfydryl-functionalized graphene oxide as ultra-high capacity adsorbent for high selectivity and ppb level removal of mercury from water under wide pH range. Environmental Pollution, 2021, 271, 116378.	3.7	18
74	Exclusive Strain Effect Boosts Overall Water Splitting in PdCu/Ir Core/Shell Nanocrystals. Angewandte Chemie, 2021, 133, 8324-8331.	1.6	18
75	Activating the MoS ₂ Basal Plane by Controllable Fabrication of Pores for an Enhanced Hydrogen Evolution Reaction. Chemistry - A European Journal, 2018, 24, 19075-19080.	1.7	17
76	Fabrication of NiC/MoC/NiMoO ₄ Heterostructured Nanorod Arrays as Stable Bifunctional Electrocatalysts for Efficient Overall Water Splitting. Chemistry - an Asian Journal, 2019, 14, 1013-1020.	1.7	17
77	Linking melem with conjugated Schiff-base bonds to boost photocatalytic efficiency of carbon nitride for overall water splitting. Nanoscale, 2021, 13, 9315-9321.	2.8	17
78	A facile solution-phase synthesis of cobalt phosphide nanorods/hollow nanoparticles. Nanoscale, 2016, 8, 4898-4902.	2.8	15
79	Structure and magnetic properties of cobalt ferrite foam with low mass density. Journal of Alloys and Compounds, 2019, 790, 947-954.	2.8	15
80	Electrochemical DNA/aptamer biosensors based on SPAAC for detection of DNA and protein. Sensors and Actuators B: Chemical, 2022, 353, 131100.	4.0	10
81	Chemical Synthesis of Magnetically Hard and Strong Rare Earth Metal Based Nanomagnets. Angewandte Chemie, 2019, 131, 612-616.	1.6	9
82	Effects of Al and Ca ions co-doping on magnetic properties of M-type strontium ferrites. Journal of Materials Science: Materials in Electronics, 2020, 31, 22375-22384.	1.1	9
83	Magnetization reversal and magnetic interactions in anisotropic Nd–Dy–Fe–Co–B/MgO/α-Fe disks and multilayers. Nanoscale, 2017, 9, 7385-7390.	2.8	8
84	NiCo layered double hydroxides derived Ni0.67Co0.33(PO3)2 as stable and efficient electrocatalysts for overall water splitting. Journal of Alloys and Compounds, 2021, 869, 159311.	2.8	8
85	In-situ synthesis of dual Z-scheme heterojunctions of cuprous oxide/layered double hydroxides/nitrogen-rich graphitic carbon nitride for photocatalytic sterilization. Journal of Colloid and Interface Science, 2022, 620, 313-321.	5.0	6
86	Structure and Magnetic Properties of Graded (001)-Oriented FePt Films Prepared by Magnetron Sputtering and Rapid Thermal Annealing. Journal of Superconductivity and Novel Magnetism, 2018, 31, 3251-3254.	0.8	3
87	In Situ Growth of Ultrafine PtPd Nanoparticles on Bifunctional NH ₂ â€Nâ€rGO with Remarkable Catalytic Activity for Ammonia Borane Dehydrogenation. ChemistrySelect, 2020, 5, 7632-7637.	0.7	3
88	Facile Synthesis of Monodisperse Pt Nanoparticles on Graphitic Carbon Nitride for Highâ€Performance Photocatalytic H ₂ evolution. ChemistrySelect, 2022, 7, .	0.7	0